Received: 21 February 2024 | Revised: 12 April 2024 | Accepted: 19 April 2024

DOI: 10.1111/cas.16207

Cancer Science WILEY

ORIGINAL ARTICLE

Circular RNA circESYT2 serves as a microRNA-665 sponge to promote the progression of hepatocellular carcinoma through ENO2

Wei Du[1] | Ying Li[1] | Xufeng Wang[1] | Sunzhe Xie[1] | Hongfei Ci[1] | Jiaming Zhou[1] | Ningqi Zhu[1] | Zule Chen[1] | Yan Zheng[2] | Huliang Jia[1,3]

[1]Hepatobiliary Surgery, Department of General Surgery, Huashan Hospital, Fudan University, Shanghai, China

[2]Department of Pancreatic Surgery, Shanghai General Hospital, Shanghai Key Laboratory of Pancreatic Disease, Institute of Pancreatic Disease, Shanghai Jiao Tong University School of Medicine, Shanghai, China

[3]Cancer Metastasis Institute, Fudan University, Shanghai, China

Correspondence
Huliang Jia, Hepatobiliary Surgery, Department of General Surgery, Huashan Hospital, Fudan University, Shanghai 200040, China.
Email: huliangjia@fudan.edu.cn

Yan Zheng, Department of Pancreatic Surgery, Shanghai General Hospital, Shanghai Key Laboratory of Pancreatic Disease, Institute of Pancreatic Disease, Shanghai Jiao Tong University School of Medicine, Shanghai 200080, China.
Email: ygziling@126.com

Funding information
National Natural Science Foundation of China, Grant/Award Number: 8187110643

Abstract

Circular RNAs (circRNAs) have emerged as crucial regulators in tumor progression, yet their specific role in hepatocellular carcinoma (HCC) remains largely uncharacterized. In this study, we utilized high-transcriptome sequencing to identify the upregulation of circESYT2 (hsa_circ_002142) in HCC tissues. Functional experiments carried out in vivo and in vitro revealed that circESYT2 played a significant role in maintaining the growth and metastatic behaviors of HCC. Through integrative analysis, we identified enolase 2 (ENO2) as a potential target regulated by circESYT2 through the competitive endogenous RNA sponge mechanism. Additional gain- or loss-of-function experiments indicated that overexpression of circESYT2 led to a tumor-promoting effect, which could be reversed by transfection of microRNA-665 (miR-665) mimic or ENO2 knockdown in HCC cells. Furthermore, the direct interaction between miR-665 and circESYT2 and between miR-665 and ENO2 was confirmed using RNA immunoprecipitation, FISH, RNA pull-down, and dual-luciferase reporter assays, highlighting the involvement of the circESYT2/miR-665/ENO2 axis in promoting HCC progression. These findings shed light on the molecular characteristics of circESYT2 in HCC tissues and suggest its potential as a biomarker or therapeutic target for HCC treatment.

KEYWORDS
ceRNA, circESYT2, ENO2, hepatocellular carcinoma progression, miR-665

Abbreviations: AGO2, argonaute 2; ceRNA, competitive endogenous RNA; circRNA, circular RNA; EMT, epithelial-to-mesenchymal transition; ENO2, enolase 2; FC, fold change; FDR, false discovery rate; HCC, hepatocellular carcinoma; IHC, immunohistochemistry; miRNA, microRNA; MUT, mutant; qRT-PCR, real-time quantitative PCR; RIP, RNA immunoprecipitation; RISC, RNA-induced silencing complex; RNA-seq, RNA sequencing; TCGA, The Cancer Genome Atlas.

Wei Du, Ying Li, and Xufeng Wang contributed equally to this work.

1 | INTRODUCTION

The global incidence of HCC is showing a gradually increasing trend.[1] With the increased mortality rate, HCC has become the third leading cause of cancer-related death worldwide, with a relative 5-year survival rate of approximately 18%.[2] China is considered a high-risk country for HCC, with approximately half of the world's new cases and deaths attributed to HCC occurring within its borders.[3] The majority of HCC patients are already in advanced stages at the time of initial diagnosis,[4] thus missing the opportunity for surgical intervention, which significantly decreases the survival rate. Therefore, it is essential to investigate the factors influencing the progression of HCC.

Circular RNAs are generated through a special splicing mechanism called back-splicing, which involves the covalent binding of the 5′-end of an upstream exon with the 3′-end of a downstream exon on the mRNA.[5] Responding to various stimulations, circRNA would possess biological functions, including serving as miRNA sponges, interacting with proteins, and coding peptides.[6] Accumulating evidence indicates that circRNA could act as a molecular sponge that exerts extensive regulatory effects in tumors.[7] However, the precise mechanisms of how circRNAs regulate the progression of HCC through ceRNA are not fully understood, highlighting the need for further investigation.

Enolase, an essential enzyme in the glycolysis process,[8] is a remarkably conserved protein that exists in archaea, bacteria,[9] and eukaryotes.[10] It catalyzes the interconversion of 2-phospho-D-glycerate and phosphoenolpyruvate, playing a necessary role in cellular energy metabolism. Enolase owns three primary isoforms: ENO1 (α-ENO), ENO2 (γ-ENO), and ENO3 (β-ENO), which show comparable enzymatic characteristics.[11] Among them, ENO2 is initially to be identified as the neuron-specific enolase,[12] which is upregulated in neural tissues and various neuroendocrine tumors (such as neuroblastoma and small-cell lung cancer).[13] Consistently, recent studies have identified elevated expression of ENO2 in other malignancies including pancreatic cancer,[14] cervical cancer,[15] renal cell carcinoma,[16] lung cancer,[17] and leukemia.[18] Especially in pancreatic cancer, ENO2 is reported to promote the sustained proliferative and invasive abilities of tumor cells through driving altered glycolysis reprogramming.[14] Although critical contributions of ENO2 have been elucidated in other tumors, the expression profile and mediatory mechanism of ENO2 in HCC remain unexplored.

In this work, we recognized a significant upregulation of circESYT2 in neoplasms with histological grade III–IV compared to those with histological grade I–II using whole transcriptome sequencing. Functional in vitro and in vivo investigations have shown that circESYT2 could boost the proliferation and migration of HCC cells. Acting as a molecular sponge for miR-665, circESYT2 weakened the suppressive impact of miR-665 on the mRNA expression of ENO2, hence promoting the advancement of HCC. The results of our research might potentially identify biomarkers that can be used for diagnosing and targeting treatments for HCC.

2 | MATERIALS AND METHODS

2.1 | Patients and samples

A total of 126 individuals diagnosed with HCC were enrolled in this study. The samples were obtained at Huashan Hospital, Fudan University, between June 2014 and December 2020 and were stored at −80°C until they were utilized.

2.2 | Supplementary methods

The methods of whole transcriptome sequencing, RNA-seq, cell culture, plasmid construction and transfection, qRT-PCR, western blot assay, RNase R digestion assay, actinomycin D assay, subcellular fraction assay, CCK-8 assay, colony formation assay, wound healing assay, trans-well assay, FISH assay, RNA pull-down, dual-luciferase reporter assay, RIPA, xenograft tumor mode and IHC, statistical analysis, the sequence of PCR primers, shRNAs, plasmid overexpression, mimics, inhibitors, and probes (Tables S1–S5) are available in Appendix S1.

3 | RESULTS

3.1 | Elevated hsa_circ_002142 expression is associated with high histological grade and bad prognosis within HCC cohort

To discover the possible involvement of circRNAs in the advancement of HCC, we undertook whole transcriptome sequencing on five human tumor samples categorized as histological grade III–IV and five tissues

FIGURE 1 Elevated hsa_circ_002142 expression is associated with high histological grade and bad prognosis within the hepatocellular carcinoma (HCC) cohort. (A) Top 10 upregulated and bottom 10 downregulated circular RNAs (circRNAs) in five histological grade III–IV HCC tissues compared with five histological grade I–II HCC tissues by whole transcriptome sequencing. CircRNAs with log2|fold change| >2 and p value <0.05 were selected as significantly different. (B) Analysis of hsa_circ_002142, hsa_circ_000897, and hsa_circ_002103 expression in 30 paired HCC tissues by real-time quantitative PCR (qRT-PCR). (C) Kaplan–Meier curves for disease-free survival based on hsa_circ_002142 expression in the Huashan cohort. $p=0.0038$. (D) Schematic illustration showing the genomic loci of the *ESYT2* gene; circESYT2 is back-spliced from exon 11 to exon 15 of ESYT2. The back-splicing site of circESYT2 was confirmed by Sanger sequencing. (E) circESYT2 was amplified from cDNA or genomic DNA from MHCC-97H and PLC cells with divergent and convergent primers, respectively. (F) qRT-PCR analysis for the resistance of circESYT2 and linear ESYT2 to RNase R in MHCC-97H and PLC cells. (G) Actinomycin D assays to evaluate the stability of circESYT2 and ESYT2 mRNA in MHCC-97H and PLC cells. (H) Nuclear-cytoplasmic fractionation and (I) FISH were carried out to examine the subcellular distribution of circESYT2 in MHCC-97H and PLC cells. 18s rRNA and U6 were used as cytoplasmic and nuclear positive controls, respectively. $^{*}p<0.05$, $^{**}p<0.01$, $^{***}p<0.001$. ns, $p>0.05$.

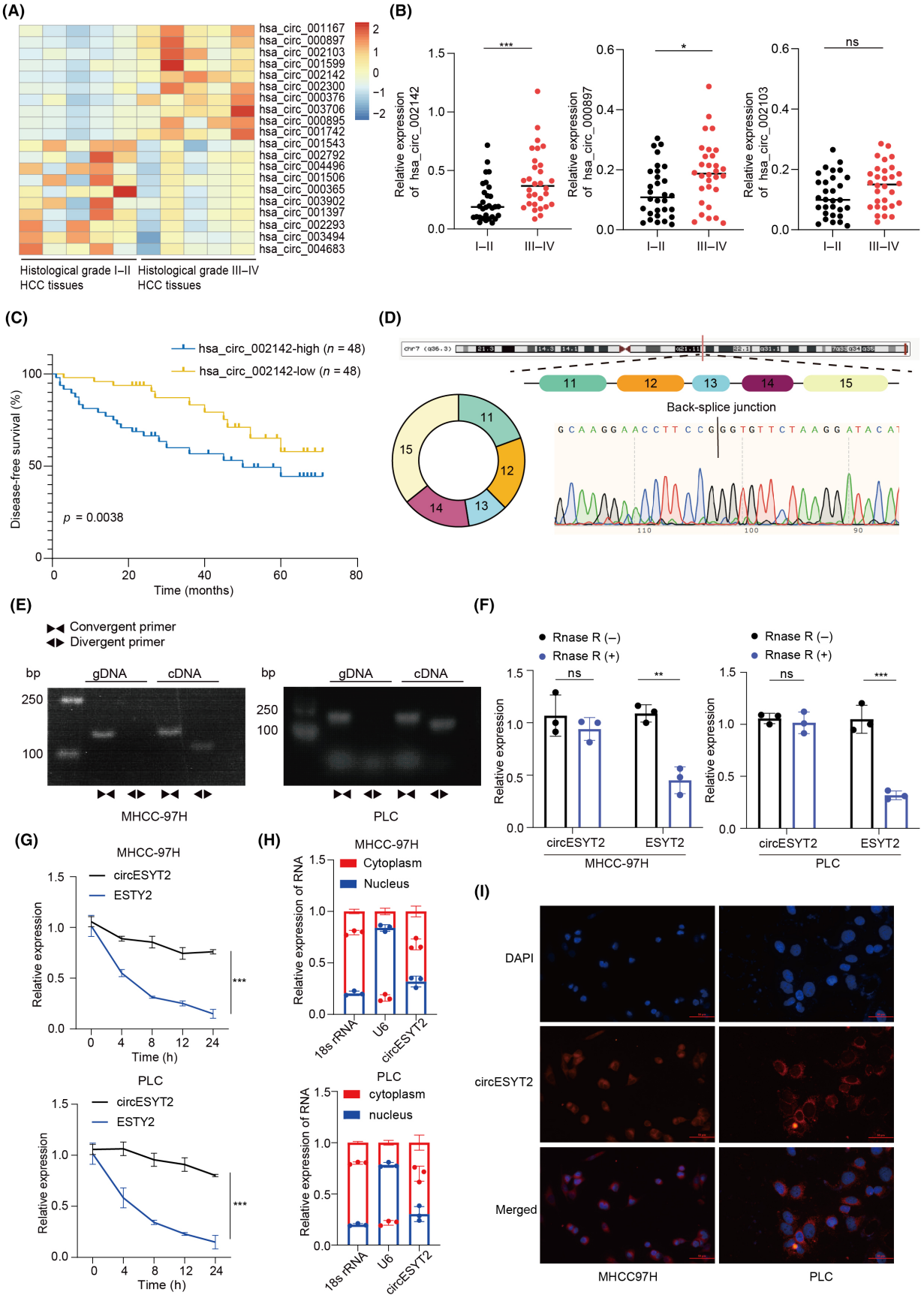
(A)
hsa_circ_001167
hsa_circ_000897
hsa_circ_002103
hsa_circ_001599
hsa_circ_002142
hsa_circ_002300
hsa_circ_000376
hsa_circ_003706
hsa_circ_000895
hsa_circ_001742
hsa_circ_001543
hsa_circ_002792
hsa_circ_004496
hsa_circ_001506
hsa_circ_000365
hsa_circ_003902
hsa_circ_001397
hsa_circ_002293
hsa_circ_003494
hsa_circ_004683
Histological grade I–II HCC tissues
Histological grade III–IV HCC tissues
(B)
Relative expression of hsa_circ_002142
Relative expression of hsa_circ_000897
Relative expression of hsa_circ_002103
I–II
III–IV
(C)
hsa_circ_002142-high (n = 48)
hsa_circ_002142-low (n = 48)
Disease-free survival (%)
p = 0.0038
Time (months)
(D)
Back-splice junction
(E)
Convergent primer
Divergent primer
bp
gDNA
cDNA
MHCC-97H
PLC
(F)
Rnase R (–)
Rnase R (+)
Relative expression
circESYT2
ESYT2
MHCC-97H
PLC
(G)
MHCC-97H
circESYT2
ESTY2
Relative expression
Time (h)
PLC
(H)
MHCC-97H
Cytoplasm
Nucleus
Relative expression of RNA
18s rRNA
U6
circESYT2
PLC
cytoplasm
nucleus
(I)
DAPI
circESYT2
Merged
MHCC97H
PLC

classified as histological grade I–II. According to the filtration criteria of log2|FC|>2 and p value <0.05, we identified 57 upregulated and 28 downregulated circRNAs in histological grade III–IV HCC tissues (Figures 1A and S1A). From the upregulated genes, further analysis with a narrowed-down p value threshold of 0.01 and utilizing the circBase[19] database led to the selection of three candidates circRNAs that had been previously detected by Salzman et al[20] or Rybak-Wolf et al,[21] including hsa_circ_000897, hsa_circ_002103, and hsa_circ_002142 (Figure S1B). Furthermore, our results illustrated that the hsa_circ_002142 mRNA level was positively correlated to the histological grade in 30 paired HCC specimens (Figure 1B). This suggested that hsa_circ_002142 could play an nonneglible regulatory role in promoting HCC progression. Subsequently, we examined the relative expression level of hsa_circ_002142 in 96 HCC tissue samples classified as histological grade III–IV. We divided the patients into high and low expression groups based on the median hsa_circ_002142 expression. Analysis of clinicopathologic parameters revealed a correlation between hsa_circ_002142 expression and tumor size as well as tumor thrombus in HCC patients (Table 1). Additionally, the Kaplan–Meier analysis indicated that the high hsa_circ_002142 group possessed a disadvantage in disease-free survival (Figure 1C). Therefore, we selected hsa_circ_002142 for further investigation.

TABLE 1 Correlation between the expression level of hsa_circ_002142 and clinicopathologic parameters in patients with histological grade III–IV hepatocellular carcinoma.

Characteristic	hsa_circ_002142 expression		p value
	Low, $n=48$	High, $n=48$	
Age (years)			
<60	27 (56)	30 (63)	0.533
≥60	21 (44)	18 (38)	
Gender			
Female	11 (23)	8 (17)	0.442
Male	37 (77)	40 (83)	
Tumor number			
Multiple	7 (15)	10 (21)	0.423
Single	41 (85)	38 (79)	
Tumor size (cm)			
≤5	28 (58)	12 (25)	<0.001
>5	20 (42)	36 (75)	
Microvascular invasion			
No	21 (44)	22 (46)	0.837
Yes	27 (56)	26 (54)	
Tumor thrombus			
No	40 (83)	24 (50)	<0.001
Yes	8 (17)	24 (50)	

Note: Data are shown as n (%).

Through an examination of the human reference genome (GRCh37/hg19), we determined that hsa_circ_002142 originates from the back-splicing of exons 11–15 of the *ESYT2* gene, which is situated on chromosome 7q36.3. The length of the sequence is 495 nt (Figure 1D). Therefore, hsa_circ_002142 was named circESYT2 according to the parental gene. Primers targeting the circular splicing site of circESYT2 were designed for PCR amplification, and Sanger sequencing confirmed the back-splicing site of circESYT2 (Figure 1D). The divergent primers specifically amplified circESYT2 only in the cDNA samples, whereas no amplification product was identified in the genomic DNA samples, validating that circESYT2 is a circular structure rather than a linear structure (Figure 1E). Moreover, RNase R digestion assays further demonstrated the resistance of circESYT2 to ribonuclease cleavage (Figure 1F). Additionally, when exposed to actinomycin D, the circESYT2 molecule showed a reduced rate of decay in comparison to the linear ESYT2 transcript, suggesting that circESYT2 has greater stability (Figure 1G). RNA subcellular fractionation and FISH assays revealed that circESYT2 is primarily localized in the cytoplasm (Figure 1H,I).

3.2 | CircESYT2 promotes proliferation and migration of HCC cells in vitro and in vivo

To elucidate the potential biological functions of circESYT2 in HCC, we examined its expression levels in commonly used cell lines. The results of qRT-PCR showed that circESYT2 was expressed at low levels in Huh7 and PLC cell lines, while it was highly expressed in MHCC-97H, HepG2, and LM3 cell lines (Figure 2A). Then the stable circESYT2 overexpressed or knocked down HCC cell lines were established. Our results showed that the shRNA and circESYT2-OE plasmid did not change the expression of linear ESYT2 (Figure 2B). Next, CCK-8 and colony formation assays indicated that the silence of circESYT2 suppressed the proliferation of MHCC-97H cells, while the overexpression of circESYT2 increased the growth rate and colony number of PLC cells (Figure 2C,D). Similarly, wound healing and Transwell migration assays showed that sh-circESYT2 weakened the migration capacity of MHCC-97H cells, whereas circESYT2 promoted the healing speed of scratch and cell migration of PLC cells (Figure 2E,F). Using western blot analysis, we observed that knockdown of circESYT2 led to a decrease in the expression levels of N-cadherin, accompanied by an increase in E-cadherin expression, while overexpression of circESYT2 yielded opposite outcomes (Figure 2G).

FIGURE 2 circESYT2 promotes the proliferation and migration of hepatocellular carcinoma (HCC) cells in vitro. (A) mRNA expression level of circESYT2 in five HCC cell lines (Huh7, PLC, MHCC-97H, HepG2, and LM3). (B) Relative RNA expression in MHCC-97H and PLC cells as indicated treatments was analyzed by real-time quantitative PCR. (C–F) Cell proliferative and migration abilities were evaluated by (C) CCK-8, (D) colony formation, (E) wound healing, and (F) Transwell migration assays in MHCC-97H and PLC cells as indicated treatments. Data are presented as means ± SD. Scale bar, 100 μm. (G) Western blot of E-cadherin and N-cadherin protein expression in MHCC-97H-shcircESYT-1/2 and PLC-circESYT2-OE cells. $^{**}p<0.01$, $^{***}p<0.001$. ns, $p>0.05$; OD450, optical density at 450 nm.

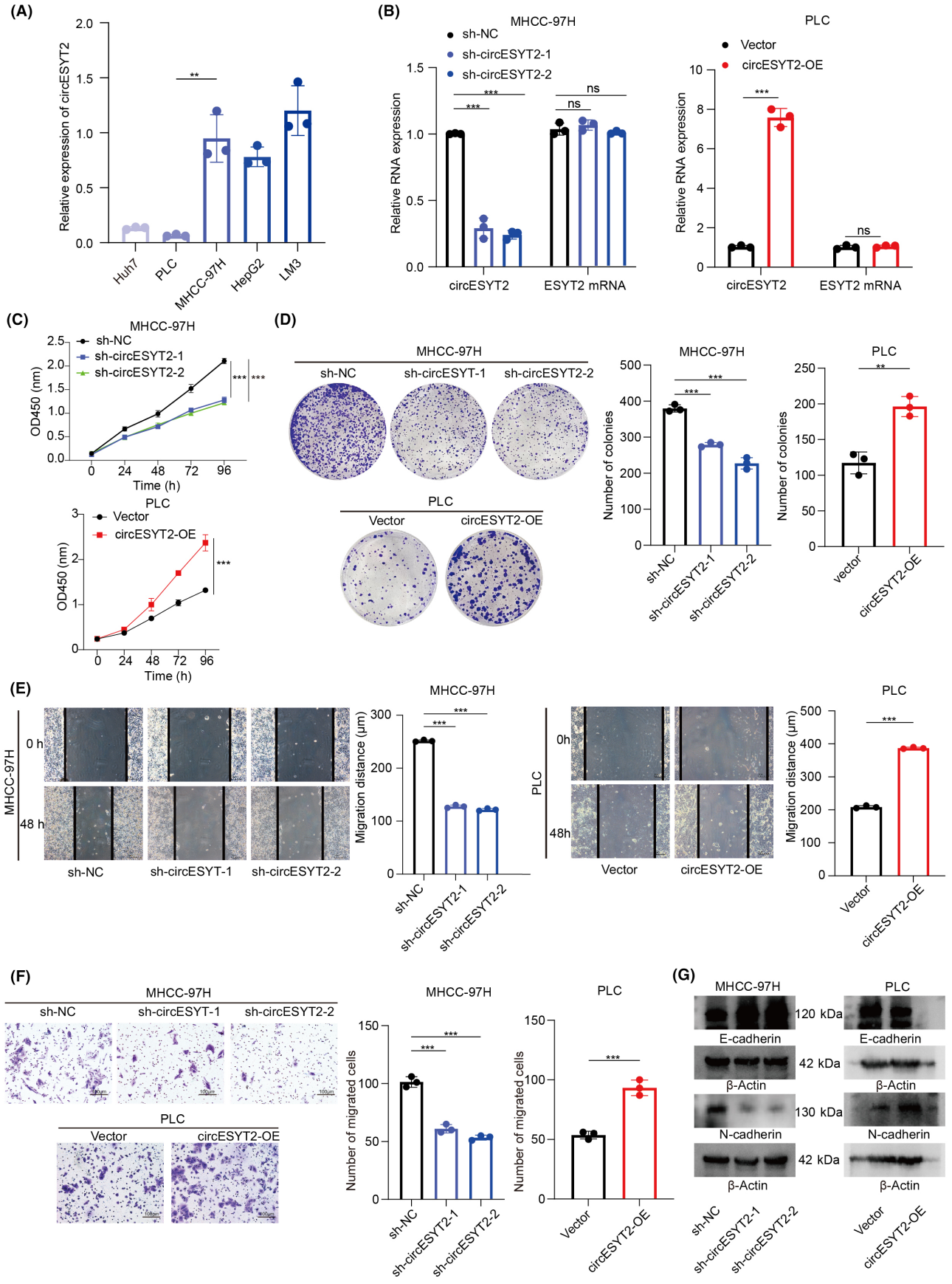
(A)
Relative expression of circESYT2
Huh7
PLC
MHCC-97H
HepG2
LM3
(B)
MHCC-97H
sh-NC
sh-circESYT2-1
sh-circESYT2-2
Relative RNA expression
circESYT2
ESYT2 mRNA
PLC
Vector
circESYT2-OE
(C)
MHCC-97H
OD450 (nm)
Time (h)
PLC
(D)
MHCC-97H
sh-NC
sh-circESYT-1
sh-circESYT2-2
PLC
Vector
circESYT2-OE
Number of colonies
(E)
MHCC-97H
0 h
48 h
Migration distance (μm)
PLC
(F)
MHCC-97H
PLC
Number of migrated cells
(G)
MHCC-97H
PLC
120 kDa
E-cadherin
42 kDa
β-Actin
130 kDa
N-cadherin

Subsequently, our findings indicate that the suppression of circESYT2 substantially hampered the proliferative capacity of MHCC97H cells in comparison to the control group in the subcutaneous HCC xenograft model (Figure 3A). Conversely, overexpression of circESYT2 in PLC cells increases the weight and growth rate of the tumor (Figure 3B). In the NCG mouse lung metastasis model, the expression of circESYT2 enabled the ability of HCC cells to metastasize to the lungs (Figure 3C). In the nude mouse liver metastasis model, knockdown of circESYT2 decreased liver metastatic lesions, while overexpression of circESYT2 led to an increase in such lesions (Figure 3D). The IHC analysis of removed tumors from nude mice showed that the knockdown of circESYT2 in HCC cells, compared to the control group, led to a decrease in the expression levels of Ki-67 and N-cadherin, accompanied by an increase in E-cadherin expression. Conversely, overexpression of circESYT2 yielded opposite outcomes (Figure 3E).

According to the above data, we proved that circESYT2 possessed the potential to prompt the malignant progression of HCC cells in vitro and in vivo.

3.3 | CircESYT2 promotes proliferation and migration of HCC cells by modulating ENO2 expression

Circular RNAs exert diverse molecular functions on the biological behavior of cancer cells by affecting protein expression through the regulatory network of ceRNAs, the interaction with proteins, or protein-coding functions.[22] To investigate the downstream molecule by which circESYT2 accelerated the progression of HCC, RNA-seq analysis was undertaken using MHCC97H-sh-NC and MHCC97H-sh-circESYT2-2 cells. Based on the selection criteria of log2|FC|>0.5 and FDR <0.05, we found that 328 genes were upregulated and 375 genes were downregulated following the knockdown of circESYT2 in MHCC-97H cells (Figure S2A,B). Furthermore, by analyzing the RNA-seq data from five histological grade III–IV HCC tissue samples versus five histological grade I–II HCC tissue samples, we identified 182 upregulated genes and 109 downregulated genes based on the criteria of log2|FC| >2 and FDR<0.001 (Figure S2C,D). Next, we intersected the downregulated genes in MHCC97H-sh-circESYT2-2 cells and the upregulated genes in the grade III–IV HCC tissue samples, revealing six genes that may be associated with circESYT2 and displayed a positive correlation. These genes are *ENO2*, *SPHK1*, *KCNN4*, *MAPK13*, *RHOV*, and *PDIA2* (Figure 4A). The qRT-PCR analysis revealed that *ENO2* mRNA level was significantly downregulated in MHCC97H cells followed by the transfection of sh-circESYT2-2 (Figure 4B) and upregulated in PLC cells transfected with circESYT2 (Figure S2E).

A study in 2020 by Zheng et al[14] confirmed that HDAC3-mediated deacetylation activates ENO2 and enhances glycolysis, promoting pancreatic cancer metastasis. Therefore, the significance of ENO2 in promoting cancer progression cannot be overlooked and its role in HCC has not been documented, thus deserving further investigation. Therefore, we first investigated the effect of ENO2 on HCC cell lines. Both transcriptionally and protein-wise, ENO2 showed low expression in PLC and Huh7 cell lines, whereas high expression was observed in MHCC-97H, HepG2, and LM3 cell lines (Figure S2F). Next, the stable ENO2 overexpressed or knocked down HCC cell lines were established (Figure S3A). The following series of experiments proved that the silencing of ENO2 suppressed the proliferation and migration capacity of MHCC-97H cells, while the overexpression of ENO2 increased the ability of PLC cells to proliferate and migrate (Figure S3B,E). Furthermore, our results indicated a significant upregulation of ENO2 expression in 30 histological grade III–IV HCC tissues compared to 30 tissues classified as grade I–II (Figure 4C). The IHC experiment also proved this point (Figure 4D). We observed a positive correlation between circESYT2 and ENO2 expression levels in 30 HCC tissues with histological grade III–IV (Figure 4E). In the TCGA database, high expression of ENO2 in HCC patients was associated with a poorer prognosis (Figure 4F).

Then we tried to determine whether circESYT2 could affect ENO2 expression. Using western blot analysis and IHC validation, we observed that knockdown of circESYT2 decreased ENO2 expression at the protein level in HCC cells and tumors from nude mice, whereas overexpression of circESYT2 increased ENO2 expression (Figure 4G,H). Next, we carried out rescue experiments to verify whether circESYT2 affected the proliferation and migration of HCC cells through ENO2. The results indicated that overexpressing ENO2 restored the proliferation and migration inhibited by sh-circESYT in MHCC-97H cells (Figure 4I–L), whereas knocking down ENO2 attenuated the enhanced the malignant behaviors of PLC cells transfected with circESYT2 (Figure S4).

These experiments reveal that circESYT2 did regulate ENO2 expression and modulate the biological functions of HCC cells through ENO2. However, the specific mechanism by which circESYT2 regulates the expression of ENO2 remains unclear.

FIGURE 3 circESYT2 promotes proliferation and migration of hepatocellular carcinoma (HCC) cells in vivo. (A, B) Xenograft tumor model was established by subcutaneously injecting circESYT2 silenced or overexpressed (OE) HCC cells. Tumor volume was measured at different time points. Tumor weight was measured after excision on the final day of the experiment. Data are presented as means ± SD. (C, D) Representative H&E staining images illustrate the metastatic abilities of MHCC-97H and PLC cells in (C) the NCG mouse model of lung metastasis and in (D) nude mouse liver metastasis following different treatments. Scale bars, 2.5 mm and 100 μm. Histograms show the number of metastatic lesions in the lungs with mean ± SD in each group. (E) Expression of Ki-67, E-cadherin, and N-cadherin in tumor by subcutaneously injecting circESYT2 silenced or overexpressed (OE) HCC cells by immunohistochemistry. Scale bar, 200 μm. $^{**}p < 0.01$, $^{***}p < 0.001$. NC, negative control.

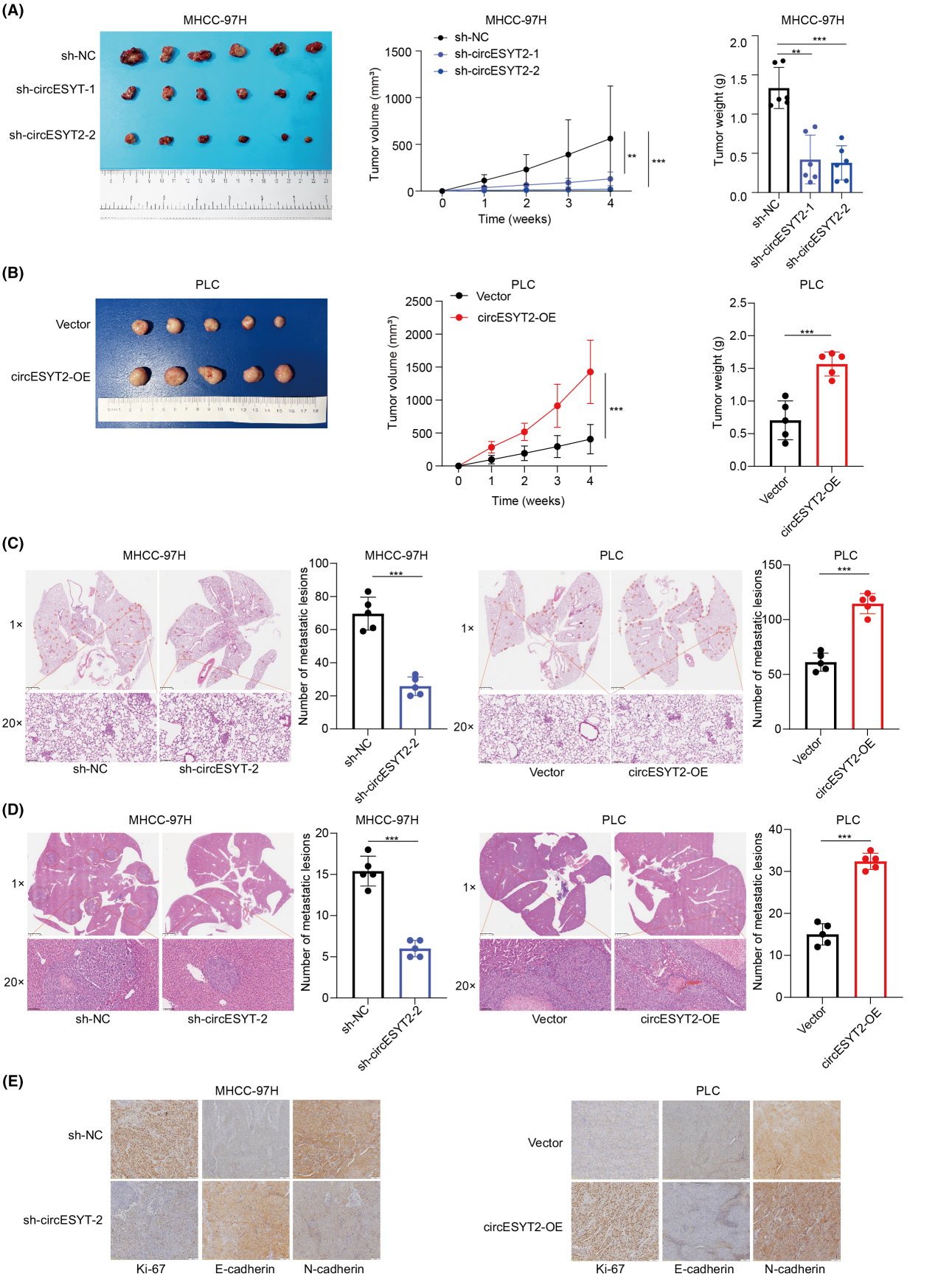
(A)
MHCC-97H
sh-NC
sh-circESYT-1
sh-circESYT2-2
MHCC-97H
sh-NC
sh-circESYT2-1
sh-circESYT2-2
Tumor volume (mm³)
Time (weeks)
MHCC-97H
Tumor weight (g)
sh-NC
sh-circESYT2-1
sh-circESYT2-2
(B)
PLC
Vector
circESYT2-OE
PLC
Vector
circESYT2-OE
Tumor volume (mm³)
Time (weeks)
PLC
Tumor weight (g)
Vector
circESYT2-OE
(C)
MHCC-97H
1×
20×
sh-NC
sh-circESYT-2
MHCC-97H
Number of metastatic lesions
sh-NC
sh-circESYT2-2
PLC
1×
20×
Vector
circESYT2-OE
PLC
Number of metastatic lesions
Vector
circESYT2-OE
(D)
MHCC-97H
1×
20×
sh-NC
sh-circESYT-2
MHCC-97H
Number of metastatic lesions
sh-NC
sh-circESYT2-2
PLC
1×
20×
Vector
circESYT2-OE
PLC
Number of metastatic lesions
Vector
circESYT2-OE
(E)
MHCC-97H
sh-NC
sh-circESYT-2
Ki-67
E-cadherin
N-cadherin
PLC
Vector
circESYT2-OE
Ki-67
E-cadherin
N-cadherin

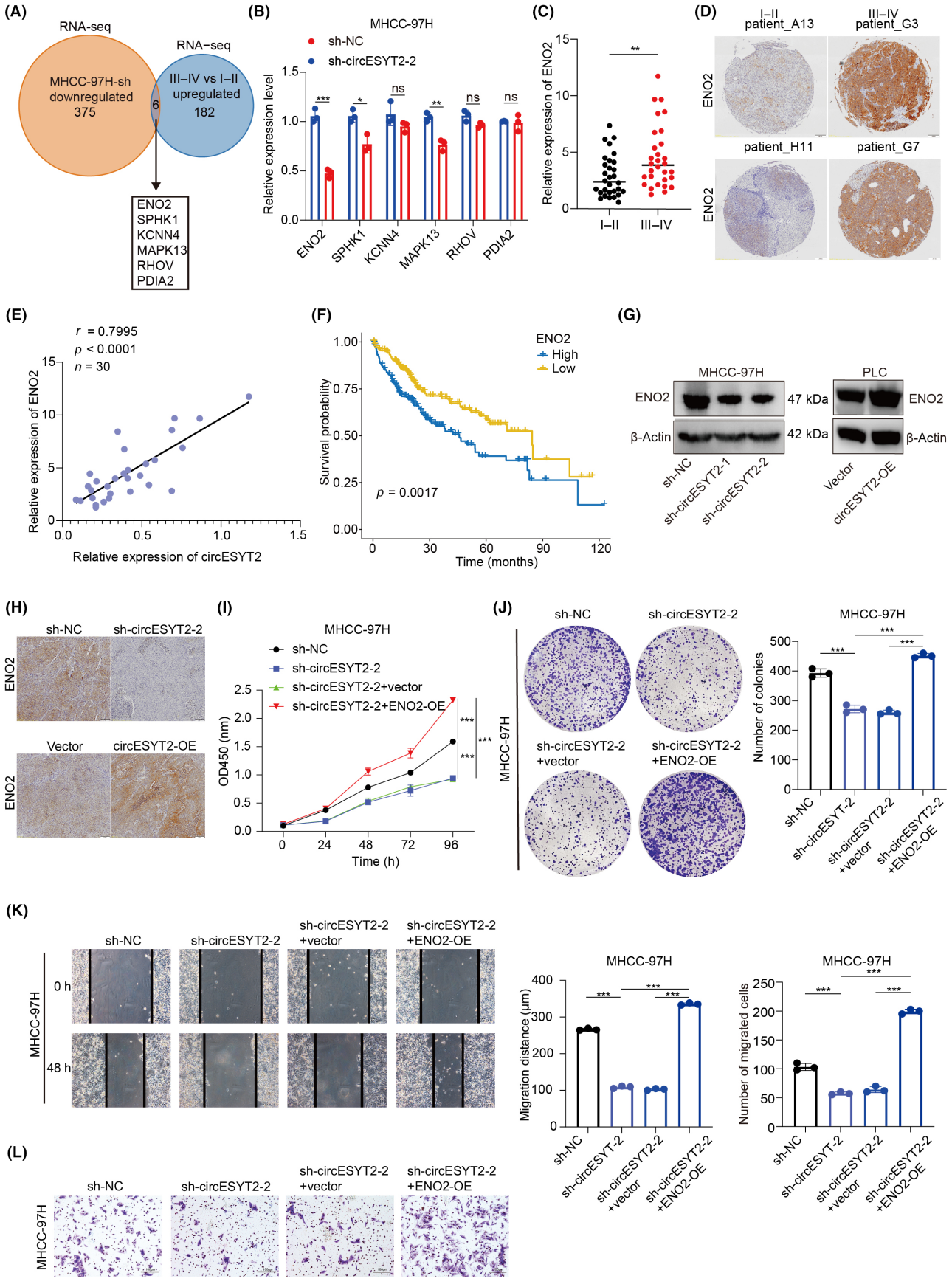
(A)
RNA-seq
MHCC-97H-sh downregulated 375
RNA−seq
III–IV vs I–II upregulated 182
6
ENO2
SPHK1
KCNN4
MAPK13
RHOV
PDIA2
(B)
MHCC-97H
sh-NC
sh-circESYT2-2
Relative expression level
ENO2
SPHK1
KCNN4
MAPK13
RHOV
PDIA2
(C)
Relative expression of ENO2
I–II
III–IV
(D)
I–II patient_A13
III–IV patient_G3
patient_H11
patient_G7
ENO2
(E)
r = 0.7995
p < 0.0001
n = 30
Relative expression of ENO2
Relative expression of circESYT2
(F)
ENO2
High
Low
Survival probability
p = 0.0017
Time (months)
(G)
MHCC-97H
PLC
ENO2
β-Actin
47 kDa
42 kDa
sh-NC
sh-circESYT2-1
sh-circESYT2-2
Vector
circESYT2-OE
(H)
sh-NC
sh-circESYT2-2
Vector
circESYT2-OE
ENO2
(I)
MHCC-97H
sh-NC
sh-circESYT2-2
sh-circESYT2-2+vector
sh-circESYT2-2+ENO2-OE
OD450 (nm)
Time (h)
(J)
sh-NC
sh-circESYT2-2
sh-circESYT2-2 +vector
sh-circESYT2-2 +ENO2-OE
MHCC-97H
Number of colonies
(K)
sh-NC
sh-circESYT2-2
sh-circESYT2-2 +vector
sh-circESYT2-2 +ENO2-OE
MHCC-97H
0 h
48 h
Migration distance (μm)
Number of migrated cells
(L)
sh-NC
sh-circESYT2-2
sh-circESYT2-2 +vector
sh-circESYT2-2 +ENO2-OE
MHCC-97H

FIGURE 4 circESYT2 promotes proliferation and migration of hepatocellular carcinoma (HCC) cells by modulating enolase 2 (ENO2) expression. (A) Venn diagram showing six potential target proteins of circESYT2. (B) Relative expression of six potential target proteins in MHCC-97H-shcircESYT2-2 cells was analyzed by real-time quantitative PCR (qRT-PCR). Data are presented as means ± SD. (C) Analysis of ENO2 expression in 30 paired HCC tissues by qRT-PCR. (D) Representative immunohistochemical staining of HCC tumors for ENO2 expression. Scale bar, 200 μm. (E) Pearson's correlation analysis of circESYT2 and ENO2 expression in 30 histological grade III–IV HCC tissues. (F) Kaplan–Meier curves for overall survival based on ENO2 expression in The Cancer Genome Atlas database. $p = 0.0017$. (G) Western blot of ENO2 protein expression in MHCC97H-shESYT2 and PLC-circESYT2-OE cells. (H) Expression of ENO2 in tumors by subcutaneously injecting circESYT2 silenced or overexpressed (OE) HCC cells by immunohistochemistry. Scale bar, 200 μm. (I, J) Cell proliferative ability detected in MHCC-97H cells with indicated treatments by (I) CCK-8 assays and (J) colony formation assays. Data are presented as means ± SD. (K, L) Cell migration ability was evaluated by (K) wound healing assays and (L) Transwell migration assays in MHCC-97H cells with indicated treatments. Scale bar, 100 μm. Data are presented as means ± SD. $^{*}p < 0.05$, $^{**}p < 0.01$, $^{***}p < 0.001$. ns, $p > 0.05$; OD450, optical density at 450 nm; RNA-seq, RNA sequencing.

3.4 | CircESYT2 acts as miR-665 sponge of ENO2 to regulate expression of ENO2

Next, we aimed to elucidate the mechanism through which circESYT2 regulated ENO2. Using the online tool CSCD (https://geneyun.net/CSCD/),[23] circESYT2 does not have the potential to interact with ENO2. According to previous studies, circRNAs predominantly localized in the cytoplasm could act as the molecular sponges of miRNAs, thereby influencing the expression and function of downstream target genes involved in tumor progression[24] through the mechanism of ceRNA.[25] Several studies have reported the involvement of circRNAs in HCC,[26] gastric cancer,[27] and bladder cancer[28] through the ceRNA mechanism. Meng et al reported that circROBO1 overexpression promotes HCC progression by regulating the miR-130a-5p/CCNT2 axis.[29] Consequently, we used the Circular RNA Interactome[30] to predict all miRNAs able to bind with circESYT2 and searched the databases TargetScanHuman[31] and miRBD[32] to predict miRNAs that possessed the interacting site on *ENO2* mRNA. The common results identified miR-665 as the only candidate miRNA capable of binding to both circESYT2 and ENO2 mRNA (Figure 5A). Then our findings revealed a significant decrease in miR-665 expression in HCC tissues classified as histological grade III-IV compared to those classified as grade I-II (Figure 5B). The evaluation of miR-665 expression in 30 HCC tissues showed a negative correlation with circESYT2 or ENO2 mRNA expression (Figure 5C,D). Using qRT-PCR, reducing the presence of circESYT2 caused an increase in the expression of miR-665, whereas increasing the presence of circESYT2 resulted in a decrease in the expression of miR-665 (Figure 5E). Subsequently, we proceeded to examine the impact of miR-665 on ENO2 expression. Validation using qRT-PCR and western blotting showed that introducing a miR-665 mimic resulted in a substantial reduction in ENO2 expression. Conversely, introducing a miR-665 inhibitor led to a rise in ENO2 expression at both the mRNA and protein levels (Figure 5F).

The mechanism of ceRNA depends on the assistance of the AGO2 protein. Processed miRNA duplexes are loaded into the RISC through interaction with the AGO2 protein in human cells.[33] In comparison with the IgG control group, a significant enrichment of circESYT2 and miR-665 was observed in the anti-AGO2 group in MHCC-97H and PLC cells, indicating that AGO2 potentially acts as a platform for the interaction between circESYT2 and miR-665 (Figures 5G and S5A). To further identify the interaction between circESYT2 and miR-665, we first predicted the binding sites between circESYT2 and miR-665 in the Circular RNA Interactome database (Figure 5H). Wild-type and corresponding MUT plasmids containing circESYT2 sequences were constructed (as shown in Figure 5I). Subsequent results of the dual-luciferase reporter assay indicated that cotransfection of WT circESYT2 plasmid and miR-665 mimic significantly reduced the activity of the firefly luciferase reporter gene compared to the negative control (miR-NC), and cotransfection of WT circESYT2 plasmid and miR-665 inhibitor significantly increased the activity of the firefly luciferase reporter gene compared to the negative control (inhibitor-NC). Cotransfection of MUT circESYT2 plasmid and miR-665 mimic or miR-665 inhibitor had no significant effect on the activity of the firefly luciferase reporter gene, indicating that circESYT2 can interact with miR-665 (Figure 5I). The subsequent dual-luciferase reporter assay results corroborated the presence of an interaction between the *ENO2* mRNA and miR-665 site (Figure 5J). Next, we confirmed their colocalization by FISH (Figure 5K) and used the RNA pull-down assay to determine the enrichment of circESYT2 using the miR-665 probe (Figure 5L). These provided further evidence for the interaction between circESYT2 and miR-665.

Based on the above results, we preliminarily confirmed that circESYT2 can sponge miR-665 through its function as a miRNA sponge. To verify whether circESYT2 affects ENO2 expression through the ceRNA mechanism by sponging miR-665, qRT-PCR and western blot analysis revealed that inhibiting miR-665 restored the ENO2 expression inhibited by sh-circESYT in MHCC-97H cells (Figure 5M), whereas overexpression of miR-665 attenuated the ENO2 expression of PLC cells transfected with circESYT2 (Figure S5B).

According to the above data, we proved that circESYT2 did regulate ENO2 expression through the ceRNA mechanism by sponging miR-665.

3.5 | CircESYT2 strengthens proliferation and migration of HCC cells through ENO2 by sponging miR-665

To further validate whether the circESYT2/miR-665/ENO2 axis promotes the progression of HCC, we carried out the following

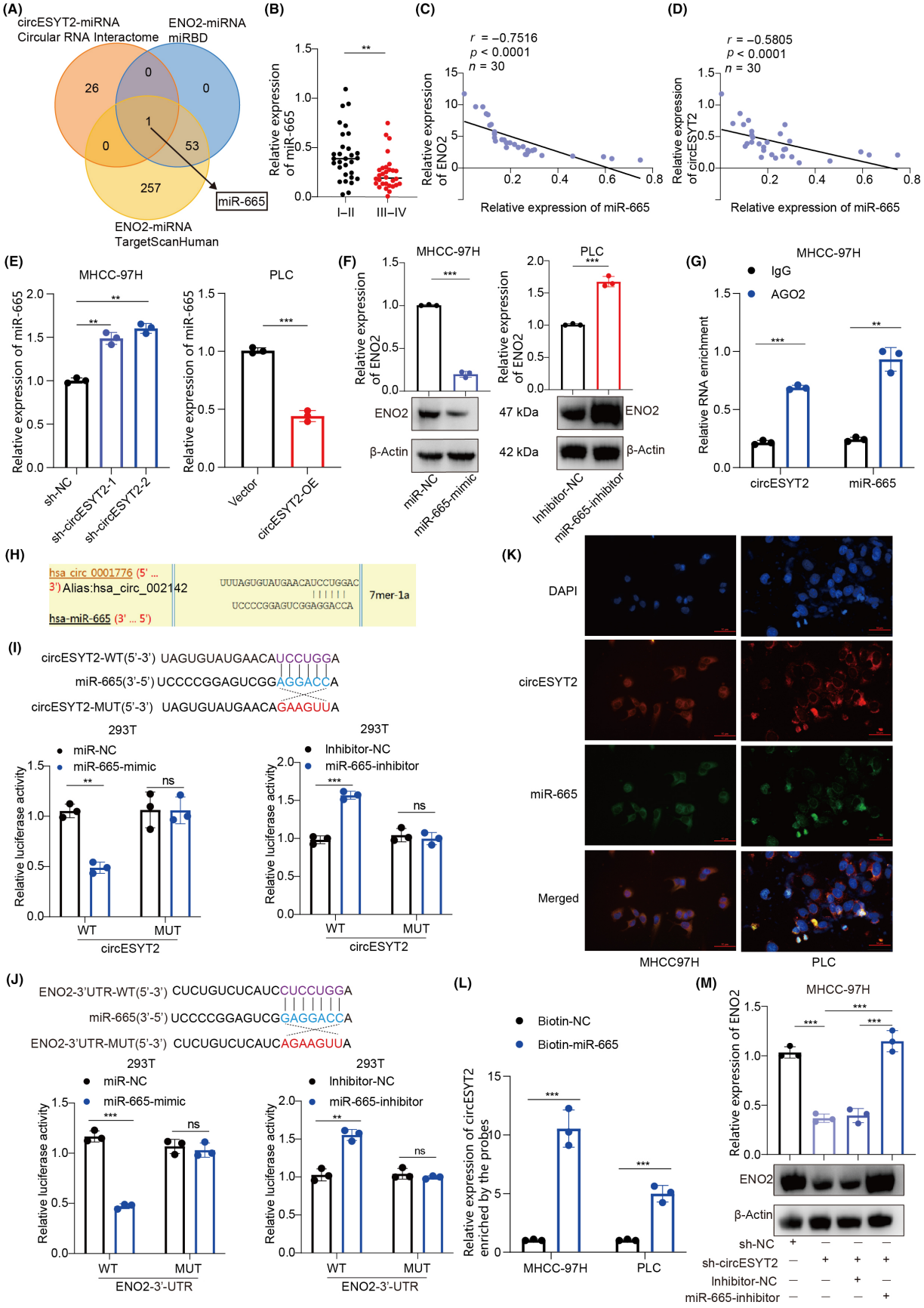
(A)
circESYT2-miRNA
Circular RNA Interactome
ENO2-miRNA
miRBD
26
0
0
1
0
53
257
miR-665
ENO2-miRNA
TargetScanHuman
(B)
Relative expression of miR-665
I–II
III–IV
(C)
r = −0.7516
p < 0.0001
n = 30
Relative expression of ENO2
Relative expression of miR-665
(D)
r = −0.5805
p < 0.0001
n = 30
Relative expression of circESYT2
Relative expression of miR-665
(E)
MHCC-97H
PLC
Relative expression of miR-665
sh-NC
sh-circESYT2-1
sh-circESYT2-2
Vector
circESYT2-OE
(F)
MHCC-97H
PLC
Relative expression of ENO2
ENO2
β-Actin
47 kDa
42 kDa
miR-NC
miR-665-mimic
Inhibitor-NC
miR-665-inhibitor
(G)
MHCC-97H
IgG
AGO2
Relative RNA enrichment
circESYT2
miR-665
(H)
hsa_circ_0001776 (5' ... 3') Alias:hsa_circ_002142
UUUAGUGUAUGAACAUCCUGGAC
UCCCCGGAGUCGGAGGACCA
7mer-1a
hsa-miR-665 (3' ... 5')
(I)
circESYT2-WT(5'-3') UAGUGUAUGAACAUCCUGGA
miR-665(3'-5') UCCCCGGAGUCGGAGGACCA
circESYT2-MUT(5'-3') UAGUGUAUGAACAGAAGUUA
293T
miR-NC
miR-665-mimic
Relative luciferase activity
WT
MUT
circESYT2
293T
Inhibitor-NC
miR-665-inhibitor
(K)
DAPI
circESYT2
miR-665
Merged
MHCC97H
PLC
(J)
ENO2-3'UTR-WT(5'-3') CUCUGUCUCAUCCUCCUGGA
miR-665(3'-5') UCCCCGGAGUCGGAGGACCA
ENO2-3'UTR-MUT(5'-3') CUCUGUCUCAUCAGAAGUUA
293T
miR-NC
miR-665-mimic
Relative luciferase activity
WT
MUT
ENO2-3'-UTR
293T
Inhibitor-NC
miR-665-inhibitor
(L)
Biotin-NC
Biotin-miR-665
Relative expression of circESYT2 enriched by the probes
MHCC-97H
PLC
(M)
MHCC-97H
Relative expression of ENO2
ENO2
β-Actin
sh-NC
sh-circESYT2
Inhibitor-NC
miR-665-inhibitor

FIGURE 5 circESYT2 acts as a microRNA-665 (miR-665) sponge of enolase 2 (ENO2) to regulate the expression of ENO2. (A) Venn diagram showing potential target miRNAs of circESYT2 and ENO2. (B) Analysis of miR-665 expression in 30 paired hepatocellular carcinoma (HCC) tissues by real-time quantitative PCR (qRT-PCR). (C, D) Pearson's correlation analysis of miR-665, circESYT2, and ENO2 expression in 30 histological grade III–IV HCC tissues. (E) Relative expression of miR-665 in MHCC-97H and PLC cells with indicated treatments was analyzed by qRT-PCR. (F) Expression of ENO2 in MHCC-97H and PLC cells with indicated treatments was analyzed by qRT-PCR and western blotting. (G) RIPA was carried out to detect circESYT2 and miR-665 binding to argonaute 2 (AGO2) in MHCC-97H cells. (H) Binding sites between circESYT2 and miR-665 were predicted using the Circular RNA Interactome database. (I) Luciferase activity of WT circESYT2 or mutant (MUT) circESYT2 after transfection with miR-665 mimic or inhibitor in MHCC-97H and PLC cells, respectively. (J) Luciferase activity of WT *ENO2* mRNA 3′-UTR or MUT *ENO2* mRNA 3′-UTR after transfection with miR-665 mimic or inhibitor in MHCC-97H and PLC cells, respectively. (K) FISH assay showed that circESYT2 (red) and miR-665 (green) colocalize in the cytoplasm. (L) RNA pull-down experiments in MHCC-97H and PLC cells confirmed that biotin-miR-665 significantly pulled down circESYT2 compared to biotin-negative control (NC). (M) Expression of ENO2 in MHCC-97H and PLC cells with indicated treatments was analyzed by qRT-PCR and western blotting. $^{**}p < 0.01$, $^{***}p < 0.001$. ns, $p > 0.05$.

experiments. First, we confirmed the impact of circESYT2 sponging miR-665 on the proliferation and migration abilities of HCC cells. The results indicated that the inhibition of miR-665 restored the proliferation and migration capabilities that were suppressed by sh-circESYT in MHCC-97H cells (Figure 6A–D). The proliferation and migration assays showed that the overexpression of miR-665 attenuated the enhanced proliferation and migration observed in PLC cells transfected with circESYT2 (Figure S6A–D). The cell proliferation and migration assays revealed that the enhanced expression of ENO2 in MHCC-97H cells, which were transfected with the miR-665 mimic, reversed the impaired proliferation and migratory capability (Figure 6E–H). Similarly, inhibiting miR-665 and knocking down ENO2 in PLC cells resulted in the reversal of the increased proliferation capacity (Figure S6E–H). These findings reinforce the notion that circESYT2 strengthens the proliferation and migration of HCC cells through ENO2 by sponging miR-665.

4 | DISCUSSION

Currently, a substantial body of research suggests that circRNAs show differential expression between individuals with HCC. These differentially expressed circRNAs may promote tumor progression and can further serve as sensitive biomarkers for cancer diagnosis and prognosis.[34] However, the molecular mechanisms underlying circRNA-mediated HCC progression remain largely unclear. In this study, we observed the upregulation of circESYT2 expression in histological grade III–IV HCC tissues compared with histological grade I–II HCC tissues. Additionally, through a combination of in vitro and in vivo experiments, we have shown that circESYT2 promotes the proliferative and invasive abilities of HCC cells. Collectively, these results provide compelling evidence for the crucial role of circESYT2 in driving the progression of HCC at the cellular level.

To investigate the potential mechanisms by which circESYT2 influences HCC progression, we intersected the downregulated genes in MHCC97H-sh-circESYT2-2 cells and the upregulated genes in the grade III–IV HCC tissue samples to identify proteins whose expression levels are most likely affected by circESYT2. Among the identified proteins, ENO2 emerged as a primary candidate. However, current research suggests that ENO2 is significantly upregulated in various tumors and is associated with poor prognosis of patients. Based on our findings, upregulation of circESYT2 resulted in a substantial elevation in ENO2 expression, thereby promoting the malignant characteristics of HCC cells. However, the precise mechanism by which circESYT2 regulates the expression of ENO2 remains elusive. Most circRNAs have been reported as ceRNAs that can sponge multiple miRNAs and inhibit their activity, thereby upregulating the expression of genes associated with these miRNAs. For example, circMET upregulates the expression of Snail through sponging miR-30-5p, thereby inducing EMT and enhancing the immunosuppressive tumor microenvironment, ultimately promoting HCC development.[35] CircTOLLIP sponged miR-516a-5p to elevate the expression of PBX3, thereby activating the EMT pathway and facilitating tumor progression in HCC.[36] Previous studies have shown that miR-665 inhibits the tumorigenesis and progression of HCC.[37] MicroRNAs function by binding to the 3′-UTR and inducing the formation of the RISC, which leads to gene degradation and inhibition of expression.[38] To further elucidate the bridging role between circESYT2 and ENO2, we attempted to find the miRNA. In our study, we found that miR-665 can interact with both circESYT2 and *ENO2* mRNA. First, we validated that the AGO2 protein provides a platform for circESYT2 to interact with miR-665. Subsequently, we showed that circESYT2 can interact with miR-665 through luciferase reporter, RNA pull-down, and FISH assays and miR-665 can interact with *ENO2* mRNA through luciferase reporter assays. Finally, we revealed that circESYT2 regulates the expression of ENO2 through miR-665. Overexpression of miR-665 attenuated the ENO2 expression of PLC cells transfected with circESYT2.

Our research findings indicated that circESYT2 can sponge endogenous miR-665 to inhibit its activity to upregulate the expression of ENO2, and further, promote the progression of HCC cells. Moreover, overexpression of miR-665 can decrease the expression level of ENO2 and suppress the promoting effects of circESYT2 on the proliferation and migration of HCC cells. These promoting effects can also be reversed upon inhibition of ENO2 expression directly. Taken together, our data indicate that circESYT2 regulates the progression of HCC through the miR-665/ENO2 pathway, providing novel insights into the role of circESYT2 in mediating HCC progression through the ceRNA regulatory network (Figure 7). circESYT2 holds promise as a novel biomarker and therapeutic target in

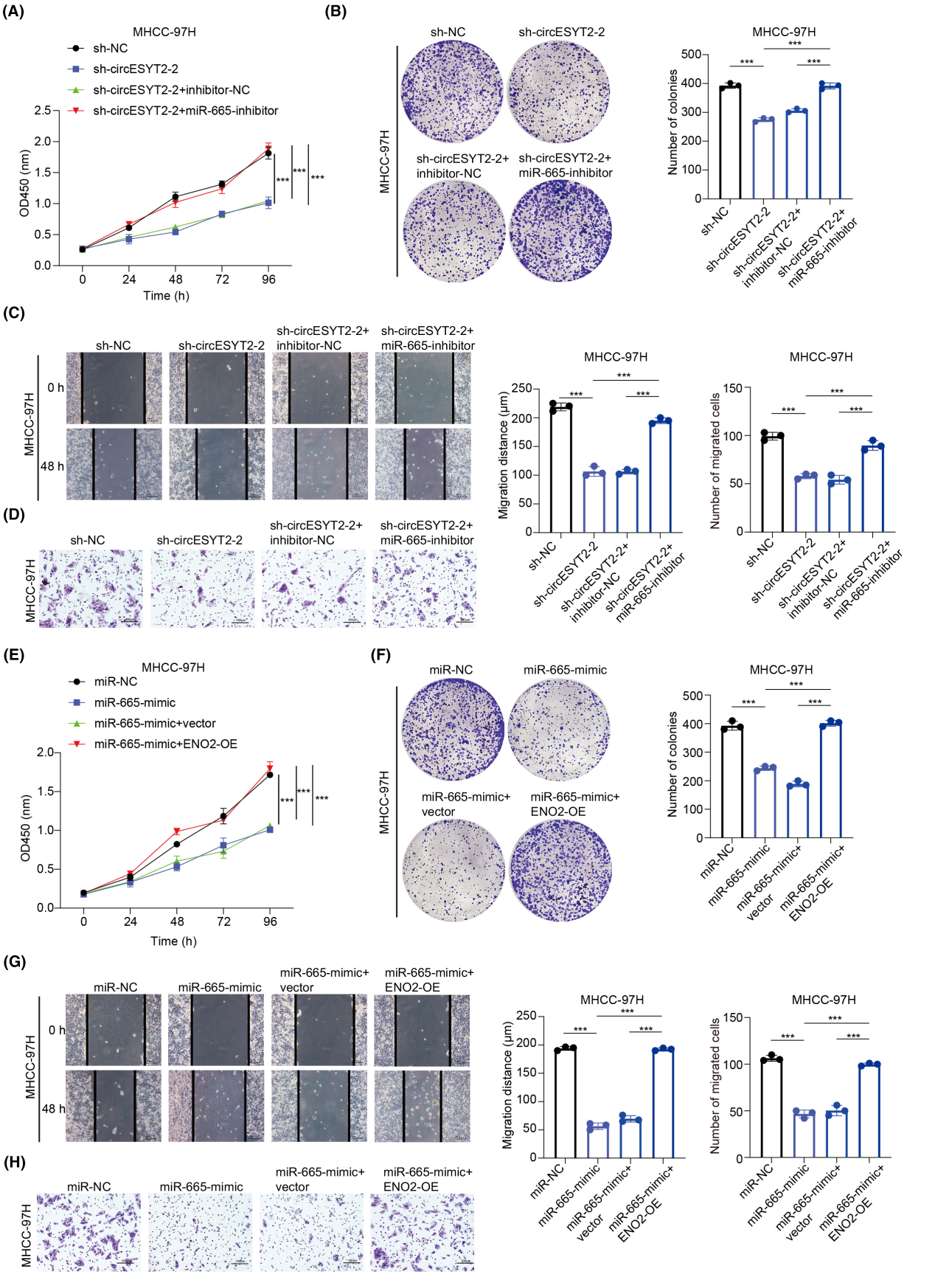

FIGURE 6 circESYT2 strengthens proliferation and migration of hepatocellular carcinoma cells through enolase 2 (ENO2) by sponging microRNA-665 (miR-665). (A–H) Cell proliferative and migration abilities were evaluated by (A, E) CCK-8, (B, F) colony formation, (C, G) wound healing, and (D, H) Transwell migration assays in MHCC-97H cells with indicated treatments. Data are presented as means ± SD. Scale bar, 100 μm. ***$p < 0.001$. NC, negative control; OD450, optical density at 450 nm; OE, overexpression.

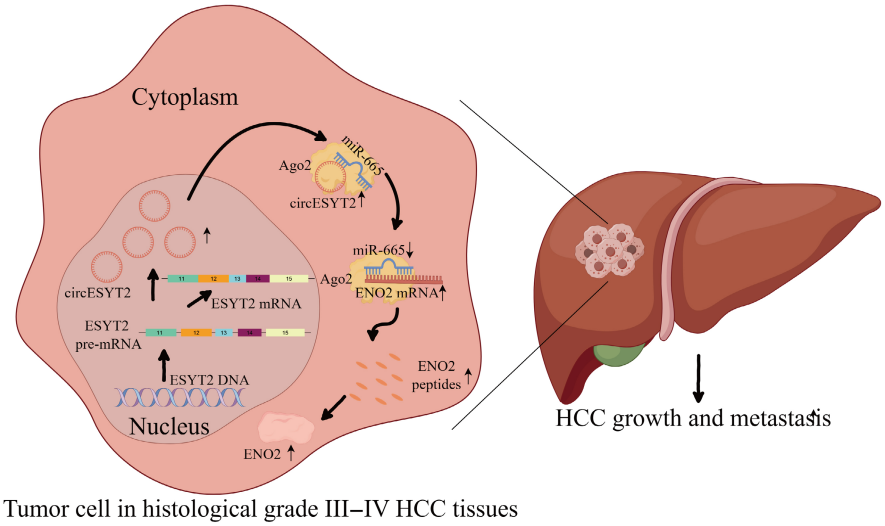

FIGURE 7 Schematic diagram of the mechanism by which circESYT2 promotes hepatocellular carcinoma (HCC) progression through regulation of the microRNA-665 (miR-665)/enolase 2 (ENO2) axis. This figure was created using the figdraw platform.

HCC. In the future, it could also be utilized as an emerging molecule for mRNA vaccines or nucleic acid drugs.

Nevertheless, our study also presents certain limitations. The specific mechanisms by which ENO2 influences the progression of HCC need further research. Furthermore, in-depth investigations are required to uncover additional functionalities of circESYT2 in HCC, including its possible functions in protein binding and encoding.

AUTHOR CONTRIBUTIONS

Wei Du: Data curation; investigation; writing – original draft; writing – review and editing. **Ying Li:** Formal analysis; methodology; writing – original draft. **Xufeng Wang:** Methodology; supervision. **Sunzhe Xie:** Methodology; supervision. **Hongfei Ci:** Validation; visualization. **Jiaming Zhou:** Investigation. **Ningqi Zhu:** Methodology. **Zule Chen:** Investigation. **Huliang Jia:** Conceptualization; funding acquisition; project administration; resources; supervision. **Yan Zheng:** Conceptualization; methodology; project administration; supervision.

ACKNOWLEDGMENTS

We would like to thank circBase, CSCD, Circular RNA Interactome, TargetScanHuman, miRBD, and TCGA databases for the availability of the data.

FUNDING INFORMATION

This study was supported by the National Natural Science Foundation of China (No. 8187110643).

CONFLICT OF INTEREST STATEMENT

The authors declare no conflict of interest.

DATA AVAILABILITY STATEMENT

Datasets used during the current study were available from the corresponding authors upon reasonable request.

ETHICS STATEMENT

Approval of the research protocol by an institutional review board: This study was approved by the Ethics Committee of Huashan Hospital, Fudan University (2018–025).

Informed consent: All procedures were conducted according to the guidelines outlined in the Declaration of Helsinki principles, and informed consent was signed by all participants.

Registry and registration no. of the study/trial: N/A.

Animal studies: All animal studies were approved by The Animal Care and Use Committee of Fudan University (2018 Huashan Hospital JS-009).

ORCID

Huliang Jia https://orcid.org/0000-0002-9782-123X

REFERENCES

1. Sung H, Ferlay J, Siegel RL, et al. Global cancer statistics 2020: GLOBOCAN estimates of incidence and mortality worldwide for 36 cancers in 185 countries. *CA Cancer J Clin*. 2021;71:209-249.
2. Siegel RL, Miller KD, Fuchs HE, Jemal A. Cancer statistics, 2022. *CA Cancer J Clin*. 2022;72:7-33.
3. Raoul J-L, Edeline J. Systemic treatment of hepatocellular carcinoma: standard of care in China and elsewhere. *Lancet Oncol*. 2020;21:479-481.
4. Llovet JM, Kelley RK, Villanueva A, et al. Hepatocellular carcinoma. *Nat Rev Dis Primers*. 2021;7:6.
5. Chen L-L. The expanding regulatory mechanisms and cellular functions of circular RNAs. *Nat Rev Mol Cell Biol*. 2020;21:475-490.
6. Zhou W-Y, Cai ZR, Liu J, Wang DS, Ju HQ, Xu RH. Circular RNA: metabolism, functions and interactions with proteins. *Mol Cancer*. 2020;19:172.
7. Lei M, Zheng G, Ning Q, Zheng J, Dong D. Translation and functional roles of circular RNAs in human cancer. *Mol Cancer*. 2020;19:30.
8. Piast M, Kustrzeba-Wójcicka I, Matusiewicz M, Banaś T. Molecular evolution of enolase. *Acta Biochim Pol*. 2005;52:507-513.
9. Morita T, Kawamoto H, Mizota T, Inada T, Aiba H. Enolase in the RNA degradosome plays a crucial role in the rapid decay of glucose transporter mRNA in the response to phosphosugar stress in Escherichia coli. *Mol Microbiol*. 2004;54:1063-1075.
10. Entelis N, Brandina I, Kamenski P, Krasheninnikov IA, Martin RP, Tarassov I. A glycolytic enzyme, enolase, is recruited as a cofactor of tRNA targeting toward mitochondria in Saccharomyces cerevisiae. *Genes Dev*. 2006;20:1609-1620.
11. Shimizu A, Suzuki F, Kato K. Characterization of alpha alpha, beta beta, gamma gamma and alpha gamma human enolase isozymes, and preparation of hybrid enolases (alpha gamma, beta gamma and alpha beta) from homodimeric forms. *Biochim Biophys Acta*. 1983;748:278-284.

12. Marangos PJ, Schmechel DE. Neuron specific enolase, a clinically useful marker for neurons and neuroendocrine cells. *Annu Rev Neurosci*. 1987;10:269-295.
13. Dong X, du Y, Zhao G, et al. Dual-signal electrochemiluminescence immunosensor for neuron-specific enolase detection based on 'dual-potential' emitter Ru(bpy)32+ functionalized zinc-based metal-organic frameworks. *Biosens Bioelectron*. 2021;192:113505.
14. Zheng Y, Wu C, Yang J, et al. Insulin-like growth factor 1-induced enolase 2 deacetylation by HDAC3 promotes metastasis of pancreatic cancer. *Signal Transduct Target Ther*. 2020;5:53.
15. Sheng J, Zhang W. Identification of biomarkers for cervical cancer in peripheral blood lymphocytes using oligonucleotide microarrays. *Chin Med J*. 2010;123:1000-1005.
16. Sun C, Liu M, Zhang W, et al. Overexpression of enolase 2 is associated with worsened prognosis and increased glycikolysis in papillary renal cell carcinoma. *J Cell Physiol*. 2021;236:3821-3831.
17. Jiang ZF, Wang M, Xu JL. Thymidine kinase 1 combined with CEA, CYFRA21-1 and NSE improved its diagnostic value for lung cancer. *Life Sci*. 2018;194:1-6.
18. Fujiwara H, Arima N, Ohtsubo H, et al. Clinical significance of serum neuron-specific enolase in patients with adult T-cell leukemia. *Am J Hematol*. 2002;71:80-84.
19. Glažar P, Papavasileiou P, Rajewsky N. circBase: a database for circular RNAs. *RNA*. 2014;20:1666-1670.
20. Salzman J, Chen RE, Olsen MN, Wang PL, Brown PO. Cell-type specific features of circular RNA expression. *PLoS Genet*. 2013;9:e1003777.
21. Rybak-Wolf A, Stottmeister C, Glažar P, et al. Circular RNAs in the mammalian brain are highly abundant, conserved, and dynamically expressed. *Mol Cell*. 2015;58:870-885.
22. Kristensen LS, Andersen MS, Stagsted LVW, Ebbesen KK, Hansen TB, Kjems J. The biogenesis, biology and characterization of circular RNAs. *Nat Rev Genet*. 2019;20:675-691.
23. Xia S, Feng J, Chen K, et al. CSCD: a database for cancer-specific circular RNAs. *Nucleic Acids Res*. 2018;46:D925-D929.
24. Li J, Sun D, Pu W, Wang J, Peng Y. Circular RNAs in cancer: biogenesis, function, and clinical significance. *Trends Cancer*. 2020;6:319-336.
25. Kristensen LS, Jakobsen T, Hager H, Kjems J. The emerging roles of circRNAs in cancer and oncology. *Nat Rev Clin Oncol*. 2022;19:188-206.
26. Louis C, Leclerc D, Coulouarn C. Emerging roles of circular RNAs in liver cancer. *JHEP Rep*. 2022;4:100413.
27. Fan H-N, Chen ZY, Chen XY, et al. METTL14-mediated m6A modification of circORC5 suppresses gastric cancer progression by regulating miR-30c-2-3p/AKT1S1 axis. *Mol Cancer*. 2022;21:51.
28. Deng G, Wang R, Sun Y, et al. Targeting androgen receptor (AR) with antiandrogen enzalutamide increases prostate cancer cell invasion yet decreases bladder cancer cell invasion via differentially altering the AR/circRNA-ARC1/miR-125b-2-3p or miR-4736/PPARγ/MMP-9 signals. *Cell Death Differ*. 2021;28:2145-2159.
29. Meng H, Li R, Xie Y, et al. Nanoparticles mediated circROBO1 silencing to inhibit hepatocellular carcinoma progression by modulating miR-130a-5p/CCNT2 Axis. *Int J Nanomedicine*. 2023;18:1677-1693.
30. Dudekula DB, Panda AC, Grammatikakis I, de S, Abdelmohsen K, Gorospe M. CircInteractome: a web tool for exploring circular RNAs and their interacting proteins and microRNAs. *RNA Biol*. 2016;13:34-42.
31. McGeary SE, Lin KS, Shi CY, et al. The biochemical basis of microRNA targeting efficacy. *Science*. 2019;366:eaav1741.
32. Chen Y, Wang X. miRDB: an online database for prediction of functional microRNA targets. *Nucleic Acids Res*. 2020;48:D127-D131.
33. Herrera-Carrillo E, Berkhout B. Dicer-independent processing of small RNA duplexes: mechanistic insights and applications. *Nucleic Acids Res*. 2017;45:10369-10379.
34. Shen H, Liu B, Xu J, et al. Circular RNAs: characteristics, biogenesis, mechanisms and functions in liver cancer. *J Hematol Oncol*. 2021;14:134.
35. Huang X-Y, Zhang PF, Wei CY, et al. Circular RNA circMET drives immunosuppression and anti-PD1 therapy resistance in hepatocellular carcinoma via the miR-30-5p/snail/DPP4 axis. *Mol Cancer*. 2020;19:92.
36. Liu Y, Song J, Zhang H, et al. EIF4A3-induced circTOLLIP promotes the progression of hepatocellular carcinoma via the miR-516a-5p/PBX3/EMT pathway. *J Exp Clin Cancer Res*. 2022;41:164.
37. Zhang T, Jing B, Bai Y, Zhang Y, Yu H. Circular RNA circTMEM45A acts as the sponge of MicroRNA-665 to promote hepatocellular carcinoma progression. *Mol Ther Nucleic Acids*. 2020;22:285-297.
38. Krol J, Loedige I, Filipowicz W. The widespread regulation of microRNA biogenesis, function and decay. *Nat Rev Genet*. 2010;11:597-610.

SUPPORTING INFORMATION

Additional supporting information can be found online in the Supporting Information section at the end of this article.

How to cite this article: Du W, Li Y, Wang X, et al. Circular RNA circESYT2 serves as a microRNA-665 sponge to promote the progression of hepatocellular carcinoma through ENO2. *Cancer Sci*. 2024;115:2659-2672. doi:10.1111/cas.16207